

# Dual-wavelength thulium-doped fibre laser based on Lyot filter incorporating intensity dependent loss mechanism

MUHAMMAD SYAUQI KUSYAIRI JAMALUS<sup>1</sup>, ABDUL HADI SULAIMAN<sup>2,\*</sup>,  
HANUN ENANI MUHAMAD ALIZA<sup>1</sup>, ABDULMOGHNI ALI WAZAE AL ALIMI<sup>3</sup>,  
SITI AZLIDA IBRAHIM<sup>4</sup>, MOHAMMED THAMER ALRESHEEDI<sup>5</sup>, ENG KHOON NG<sup>6</sup>,  
MOHD ADZIR MAHDI<sup>3,7</sup>, NELIDYA MD YUSOFF<sup>1,\*</sup>

<sup>1</sup>Faculty of Artificial Intelligence, Universiti Teknologi Malaysia, Jalan Sultan Yahya Petra, 54100, Kuala Lumpur, Malaysia

<sup>2</sup>School of Physics, Universiti Sains Malaysia, 11800 Gelugor, Penang, Malaysia

<sup>3</sup>Institute of Nanoscience and Nanotechnology (ION2), Universiti Putra Malaysia, 43400 UPM Serdang, Selangor, Malaysia

<sup>4</sup>Faculty of Engineering, Multimedia University, Persiaran Multimedia 63100, Selangor, Cyberjaya, Malaysia

<sup>5</sup>Department of Electrical Engineering, College of Engineering, P.O. Box 800, King Saud University, Riyadh 11421, Kingdom of Saudi Arabia

<sup>6</sup>Department of Engineering, University of Cambridge, Cambridge, CB3 0FA, United Kingdom

<sup>7</sup>Wireless and Photonics Networks Research Center, Faculty of Engineering, Universiti Putra Malaysia, 43400 UPM Serdang, Selangor, Malaysia

---

A dual-wavelength thulium-doped fiber laser based on Lyot filter is demonstrated experimentally. A combination of highly nonlinear fiber and a polarizer is applied to induce an intensity-dependent loss mechanism in the laser cavity to suppress homogeneous gain broadening to generate a stable dual output. Upon applying different polarization-maintaining fiber lengths, the wavelength spacing can be changed from 1.8 nm to 0.6 nm. The extinction ratio for the dual lasers is high around 40 dB. The output power is stable with variation of 2.60 dB and 4.69 dB for each channel.

(Received November 5, 2024; accepted April 15, 2025)

**Keywords:** Thulium-doped fiber laser, Dual-wavelength fiber laser, Lyot filter, Intensity-dependent loss

---

## 1. Introduction

Multiwavelength fiber lasers (MWFLs) have been getting a lot of attention in fields such as optical communication, spectroscopy and optical sensing [1–3] due to its advantages such as a wide tunable range, narrow linewidth and compact structure [4–6]. Apart of MWFLs, erbium doped fiber lasers (EDFLs) have been focused on the 1.5  $\mu\text{m}$  wavelength region, which extends from 1535 nm to 1620 nm. In the other hand, thulium-doped fiber lasers (TDFLs) operate in the eye-safe 2  $\mu\text{m}$  region, typically located in the 1.7–2.1  $\mu\text{m}$  region [7]. This trait helps in the applications of TDFL of biomedical treatment [8–10], remote sensing [11] and light detection and ranging [12]. However, realizing a stable MWFL has some difficulties because of the homogeneous gain broadening in the gain medium [13–15]. Therefore, researchers have come up with numerous methods to cope with the gain mode competition in the gain-broadened medium: inducing an intensity dependent loss (IDL) mechanism [15–17] cascaded four-wave mixing (FWM) effect [6,14]. W. HE et al. implemented the IDL mechanism to control

the signal's polarization state in their tunable multiwavelength TDFL [16]. They obtained a 3-dB linewidth value of 0.4 nm and a side-mode suppression ratio (SMSR) of more than 32.4 dB. X. WANG et al. incorporated stimulated Brillouin scattering and IDL mechanism which resulted in a wavelength shift of less than 0.01 nm and peak power fluctuations of less than 0.5 dB in their multiwavelength TDFL [6]. H. Ahmad et al. used the FWM effect by including a highly nonlinear fiber (HNLF) in their configuration of a TDFL. The outcome of this approach is a wavelength shift of less than 0.05 nm and power fluctuations of less than 2.8 dB [14]. L. Zhu et al. included a Sagnac loop mirror in their TDFL configuration. They obtained a wavelength shift and power variation of 0.15 nm and 2.1 dB, respectively, on top of an SMSR of more than 26 dB [18].

Other comb filters were utilized for multiwavelength generation based on TDFL such as Mach-Zehnder interferometer (MZI) [4], Lyot filter [15,19] and Fabry-Perot interferometer [20] are just a few of the notable optical filters used in fiber lasers. P. Zhang et al. used an MZI in TDFL setup and obtained stable multiwavelength

spectra with wavelength shifts and peak power fluctuations of less than  $\pm 0.02$  nm and  $\pm 0.5$  dB, respectively [4]. Besides, the Fabry Perot interferometer was used by Y. Wei et al., as their wavelength-tunable TDFL presented a tunable signal ranging from 1940 to 2010 nm and an extinction ratio (ER) of higher than 50 dB at 800 mW of pump power [21]. Another fiber structure is Lyot filter based on polarization-maintaining fiber (PMF), which has been widely applied due to its flexibility, simple structure, and good stability [15,19]. For example, S. Liu et al. attained multiwavelength TDFL with output power variations of 0.237 dB and wavelength shift of 0.055 nm by using a Lyot filter [15]. Y. Wei et al. utilized a Lyot filter in their work where they achieved a TDFL with channel-spacing tunable abilities [22]. They managed to obtain a multiwavelength TDFL with a wavelength range of 12 nm from 1960 to 1972 nm. Using a fixed pump power of 3 W, an ER of approximately 30 dB was achieved the peak power fluctuation is around 1 dB.

Another component in generating dual-wavelength fiber laser (DWFL) is a comb filter. Previously, the DWFLs were demonstrated by utilizing comb filters such as a polarization-maintaining erbium-doped fiber (PM-

EDF) [23], Lyot filter [7,24], stimulated Raman scattering [25] and fiber Bragg grating (FBG) [26–28]. Moreover, methods such as incorporating a spectral filtering effect [29], Fabry-Perot interferometer [30], two series of FBGs [31] and compound filters such as a dual pass-Mach-Zehnder interferometer-PMF filter with transmission type of ring filter [32] and Lyot-Sagnac [33] could also be used as comb filters in DWFLs. For instance, N. MD. Yusoff et al. incorporated PM-EDF and IDL mechanism to further enhance the polarization hole burning method and suppress mode competition in the gain medium [34]. H. ZOU et al. constructed a compound filter by combining a double pass MZI-PMF filter with TTR [32]. Another DWFL was demonstrated by M. Ummay et al. when they used FBG and a tunable thin film-based filter as a wavelength selection tool and a C-band semiconductor optical amplifier (SOA) as a gain medium [35]. A DWFL using a TDF as gain medium was demonstrated by A. W. Al-Alimi et al. [7]. Using a tapered optical fiber as a comb filter, they managed to achieve a peak power fluctuation of less than 3 dB. From the best of our knowledge, it is hard to find research on DWFL-based thulium doped fiber amplifier (TDFA) utilizing IDL mechanism.

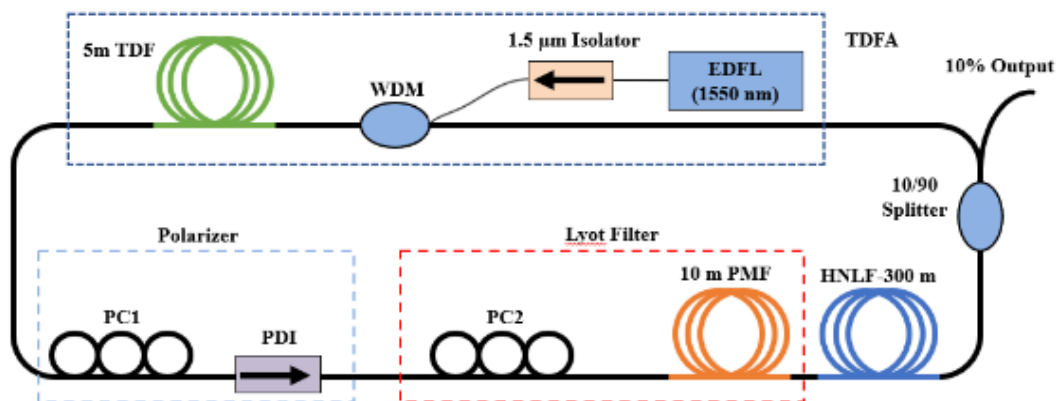


Fig. 1. The experimental setup of DWTFDL based on a Lyot filter (colour online)

In this paper, we have demonstrated dual-wavelength TDFL (DWTFDL) based on the Lyot filter with the assistance of the IDL mechanism. The IDL mechanism is induced by HNLF and polarizer to alleviate the mode competition caused by homogeneous gain broadening in EDF. Three different wavelengths spacing is demonstrated due to the use of different PMF lengths. The 5, 10 and 15 m PMF produce wavelength spacing of 1.8, 0.9 and 0.6 nm, respectively. The multiwavelength generation with 10 m PMF is more stable than other PMF lengths. A dual-wavelength spectrum at 1934.5 and 1935.4 nm was obtained with a wavelength shift of 0.5 nm. The output channel at 1934.5 nm has a power variation of 2.60 dB and the output channel 1935.4 nm has a power variation of 4.69 dB. The other two PMF lengths exhibit high values in terms of wavelength shift and power variation

## 2. Experimental setup

Fig. 1 illustrates the configuration of a TDFL based on a parallel Lyot filter. In the setup, an EDFA model CEFL-TERA with narrow linewidth is the first device of TDFA which used as a 1550 nm pump source. Pumping at 1550 nm allows for in-band pumping schemes that are spectrally closer to the desired emission wavelengths, facilitating more efficient energy transfer and reducing the thermal load on the fiber. Furthermore, operating at shorter wavelengths within the thulium emission spectrum can lead to significant reabsorption losses due to the quasi-three-level nature of the transition. In-band pumping at 1550 nm mitigates these losses, enhancing overall efficiency [36]. A 1.5 μm isolator is connected after the EDFA to ensure the one-way direction of the pump signal into the cavity and avoid any back reflection to the EDFA. Then, a 1550/2000 nm wavelength division multiplexer (WDM) coupler combines the pump signal and the oscillating signal in the ring cavity. The last component of

TDF is a 5 m TDF (OFS, TmDF200) with a peak absorption of 200 dB/m at 790 nm, numerical aperture of  $0.26 \pm 0.02$  and a cut-off wavelength of 1350 nm. A combination of polarization controller 1 (PC1) and polarization dependent isolator (PDI) forms a polarizer. The PDI is used to provide an output of linearly polarized light and create unidirectional propagation in an anti-clockwise direction. The PC1 is adjusted to ensure a proper polarization state and angle is obtained before entering the PDI for the best operation of PDI of linearly polarized light. Next, a Lyot filter which acts as a comb filter is included in the laser cavity, which consists of PC2 and a spool of PMF. Since the multiwavelength oscillation is in one direction (anti-clockwise direction), only one PC is enough for the construction of the Lyot filter. A combination of polarizer and HNLF increases the strength of an IDL mechanism in the laser cavity to stabilize and flatten the laser wavelengths [36]. The 90% port of the 10/90 splitter is connected to the WDM coupler to maintain the light oscillation within the cavity, while the 10% port is connected to an optical spectrum analyzer (OSA) from Yokogawa, model no AQ6375B with 0.05 nm resolution

### 3. Principle of operation

NPR effect could be defined as a phenomenon where the optical intensity can determine the change of a light's polarization direction in a fiber [38]. The NPR effect is useful in fiber lasers as it suppresses the mode competition and produces a more stable multiwavelength output [39]. At a certain degree and state of polarization state, an IDL mechanism is induced, as the mechanism is crucial in flattening and providing stability in our DWTDFL. When a signal propagates through a Lyot filter, the PC adjusts the polarization angle so the signal can equally enter the slow and fast axis of the PMF at the same amplitude and PS. The PC is adjusted to ensure the light entering PMF has a  $45^\circ$  angle concerning the polarization axis of the PMF. With the  $45^\circ$  angle, the light splits orthogonally into two polarization components along those polarization axes at different speeds. The two propagated lights now have the same amplitude and PS and combine in phase at the PMF's end, resulting in twice the original amplitude at the same wavelength. This phenomenon known as constructive interference explains the generation of a multiwavelength spectrum. It must be reiterated that the PC must be adjusted properly. Otherwise, different PS and amplitude values of the signal will enter the slow and fast axis of the PMF. This, in turn, will deter multiwavelength performance. The wavelength spacing between the generated wavelengths,  $\Delta\lambda$ , can be calculated by using Equation (1) below, where  $\lambda$  is the transmission wavelength, B is the birefringence of the PMF (with a value of  $4.1 \times 10^{-4}$ ) and L is the PMF length [40].

$$\Delta\lambda = \lambda^2 / BL \quad (1)$$

### 4. Results and discussion

In this experiment, three different PMF lengths were used at 5 m, 10 m and 15 m to demonstrate three different wavelength spacings. At first, we characterized the multiwavelength operation at different pump powers. The pump power is changed from 300 mW to 900 mW for three different PMF lengths while the PS of the PCs is fixed. Fig. 2(a) illustrates the output powers at different wavelengths as a function of pump power for a 5 m PMF. A clear spectrum appeared at a low pump power of 300 mW, since lasing does not start until 350 mW, that explains why there are no lasing lines at 300 mW as the lasing threshold has not yet been reached. At 400 mW, a dual-wavelength is released at 1916.1 nm and 1917.9 nm with peak powers of -27.85 dBm and -24.51 dBm, respectively. The dual-wavelength has a wavelength spacing of 1.8 nm corresponding to the PMF length. The power of the generated dual-wavelength significantly improved as pump power increases. However, the dual-wavelength is shifted to longer wavelength for pump power of higher than 400 mW. For instance, wavelengths of 1928.1 nm and 1929.9 nm with power of -34.59 dBm and -32.60 dBm, respectively, are obtained at a pump power of 500 mW. This is due to the fact that during the adjustment process, there is a degree of randomness to the polarization states [38]. When the pump powers are increased, the polarization states change which explains the big wavelength shift when the pump power was increased from 400 mW to 500 mW.

Different sets of dual wavelengths also obtained as the pump power is further increased. At 600 mW, a dual-wavelength spectrum at 1927.9 nm and 1929.7 nm with output power values of -26.73 dBm and -29.89 dBm, respectively is obtained. Including these results, the relevant graph for different sets of dual-wavelength spectrum generation for pump power of 400 - 900 mW is presented in Fig. 2. Findings show the direct proportionality between the power and pump power. A maximum output power of -21.12 dBm and -16.61 dBm at 1927.8 nm and 1929.6 nm, respectively, are obtained at 900 mW pump power.

Similarly, the dual-wavelength spectra for using a 10 m PMF in the TDFL based on a single Lyot filter setup is shown in Fig. 2(b). At 300 mW, lasing had not occurred as the lasing threshold had not surpassed the 350 mW threshold mentioned earlier. Thulium ions have relatively low absorption cross-sections at common pump wavelengths [41]. If the pump wavelength is not properly matched to the absorption peak, a substantial amount of pump power may be needed to achieve the lasing threshold. Additionally, optical losses from fiber splicing, connectors and optical components can further increase the threshold power. At 400 mW, a dual-wavelength result was obtained at the output powers of -24.88 and -24.14 dBm at 1935.0 and 1935.9 nm, respectively, meaning the wavelength spacing for using a 10 m PMF is 0.9 nm. The output power increased to -19.44 nm and -19.27 dBm at 1934.8 nm and 1935.7 nm, respectively at 500 mW but the output power decreased to -25.66 and -25.83 dBm at

1934.7 and 1935.6 nm, respectively at 600 mW. This might be due to several reasons such as the temperature fluctuation of the fiber or the vibrations affecting the experimental setup. The output power of lasing lines increased at 700 mW with -21.46 dBm and -21.83 dBm values at 1934.7 nm and 1935.6 nm, respectively. Finally, the output power of the lasing lines increased again at 800 mW. At 1934.8 nm and 1935.7 nm the output powers were -14.30 dBm and -12.41 dBm, respectively. The maximum output power was obtained at 900 mW with -11.33 dBm and 11.83 dBm values at 1934.2 nm and 1935.1 nm, respectively.

The spectra from using a 15 m PMF in the TDFL based on a single Lyot filter is depicted in Fig. 2(c). At 400 mW, a dual wavelength is obtained with peak powers of -35.99 dBm and -35.67 dBm at 1922.7 nm and 1923.3 nm, respectively. We can note that the wavelength spacing after using a 15 m PMF is 0.6 nm. The output power increased as the pump power was increased. The peak

output power increased to -18.37 dBm and -18.89 dBm at 1922.8 and 1923.4 nm, respectively when the pump power was increased to 500 mW. At 600 mW, peak powers of -15.27 dBm and -15.33 dBm were obtained at 1922.8 nm and 1923.4 nm. The output power increased again slightly at 700 mW pump power. At 1922.8 nm and 1923.4 nm, the output powers were -14.85 dBm and -14.16 dBm, respectively. However, the peak powers decreased slightly at 800 mW pump power with -16.79 dBm and -14.81 dBm values at 1922.9 nm and 1923.5 nm, respectively. Finally, the maximum output power was obtained at 900 mW with -12.31 dBm and -10.35 dBm at wavelengths 1922.5 nm and 1923.1 nm, respectively. For the phenomenon in Fig. 2, vibrations and temperature of surroundings can destabilize the polarization state and therefore affect the gain mode competition and result in power fluctuations of wavelengths, disrupting the performance of a fiber laser and causing the peak power value to decrease [41].

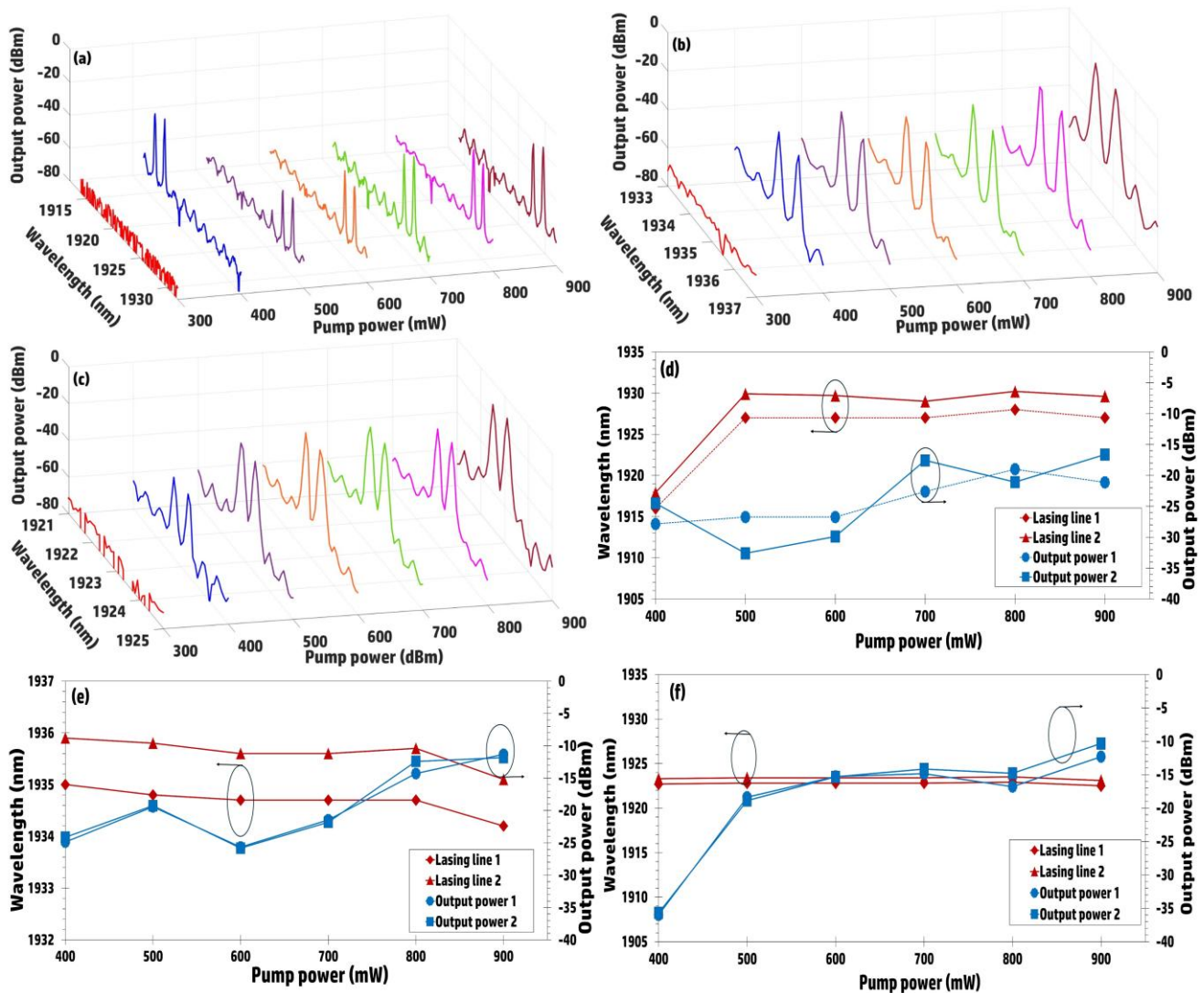


Fig. 2. Output power spectra of DWTDFL based on a single Lyot filter using (a) 5 m, (b) 10 m and (c) 15 m PMF at varying pump powers. The wavelength shifting and output power with pump power increment at PMF length (d) 5 m, (e) 10 m and (f) 15 m (colour online)

Further analysis is implemented by investigating the effects of changing the half-wave plate (HWP) of PC2 on the TDFL performance for different PMF lengths of 5 m, 10 m and 15 m PMF as shown in Fig. 3(a)-(c). In this investigation, the PC is adjusted to obtain the highest ER of generated dual-wavelength for all three PMF lengths. For the 5 m PMF, one set of dual-wavelength spectrums is only achieved with a HWP angle of  $80^\circ$  as presented in Fig. 3(a). In contrast, with 10 m PMF, 3 lasing lines may have been obtained at  $0^\circ$  of HWP but the spectrum is not flat as the power variation is over 10 dB. However, by continuously adjusting the angle of HWP a flat channel can be obtained. A dual-wavelength spectrum with peak powers of  $-22.57$  dBm and  $-23.29$  dBm at  $1946.5$  nm and  $1947.4$  nm, respectively, was obtained at an HWP angle of  $20^\circ$ . Other sets of dual-wavelength spectra can be obtained as the angle of HWP is adjusted from  $80^\circ$  to  $180^\circ$  as shown in Fig. 3(b). Fig. 3(c) shows the output spectra for 15 m of PMF at different angles of HWP. From the figures, a dual-wavelength spectrum is obtained at  $60^\circ$  and  $160^\circ$ . The laser can be switched to a single line at  $120^\circ$ ,

$140^\circ$  and  $180^\circ$ . When the HWP angle shifts, the polarization state changes. The change in polarization state causes the absence of a dual-wavelength spectrum at other HWP angles.

Fig. 4(a)-(c) shows the typical spectra of the DWTDFL at 900 mW pump power for 5, 10 and 15 m PMF with HWP angles of  $80^\circ$ ,  $20^\circ$  and  $60^\circ$ , respectively. The figures present the ER along with the wavelength spacing for each PMF length. The 5 m, 10 m and 15 m PMFs have wavelength spacings of 1.8, 0.9 and 0.6 nm, respectively. The highest ER was obtained using the 15 m PMF which is 45.19 dB, compared to 42.31 dB and 37.47 dB for 5 m and 10 m PMF, respectively. ASE is higher at the lower pump power values. Thus, the noise floor is higher which results in lowering the ER. However, instead of gradually increasing, Fig. 4 shows that the ER values for each PMF length seem to fluctuate when the pump power increases. It is believed that the surroundings of the experiment may affect the results of the ER. Vibrations and temperature of the surroundings, among other factors, may cause fluctuations of the ER [41].

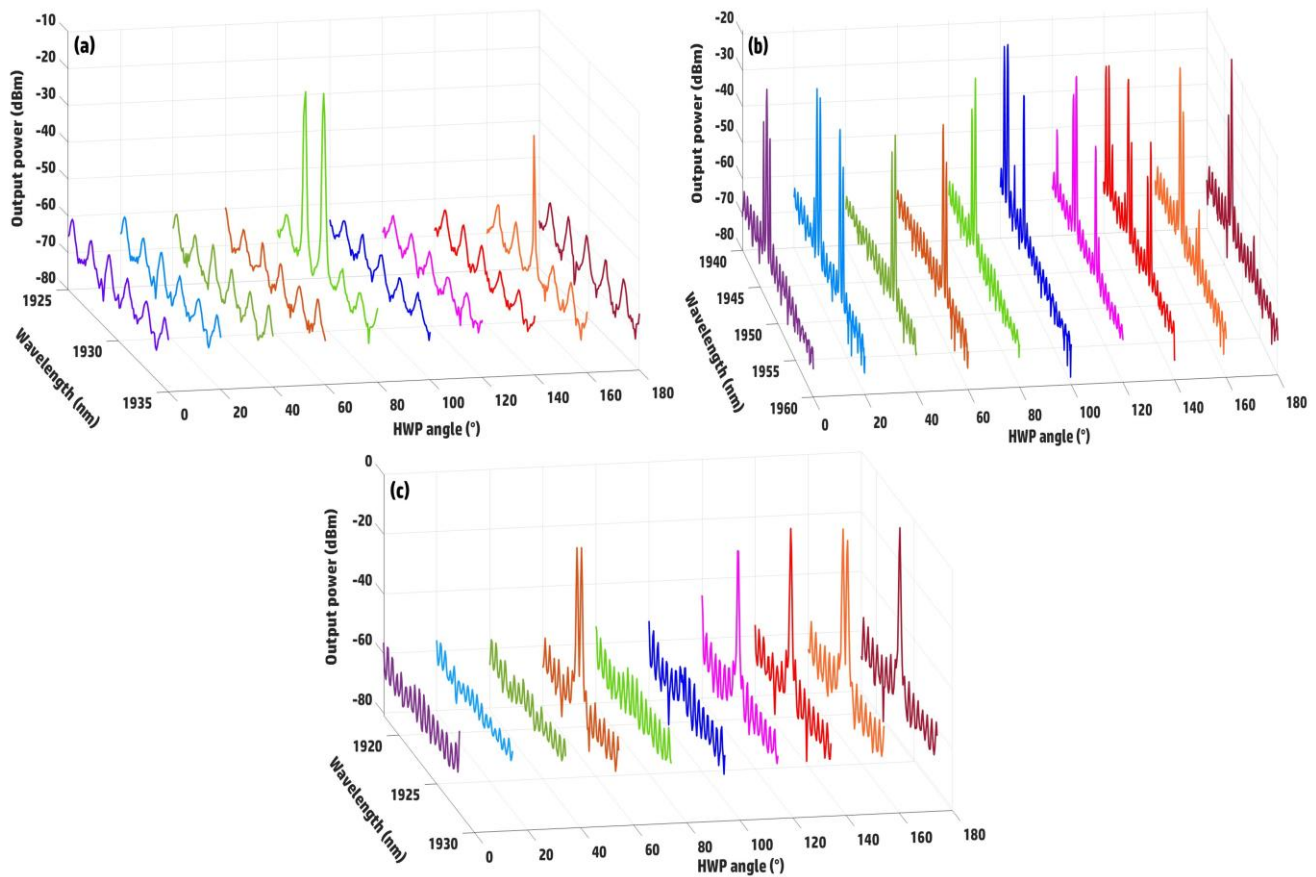


Fig. 3. The spectra at PMF lengths of (a) 5 m, (b) 10 m and (c) 15 m at various HWP angles (colour online)

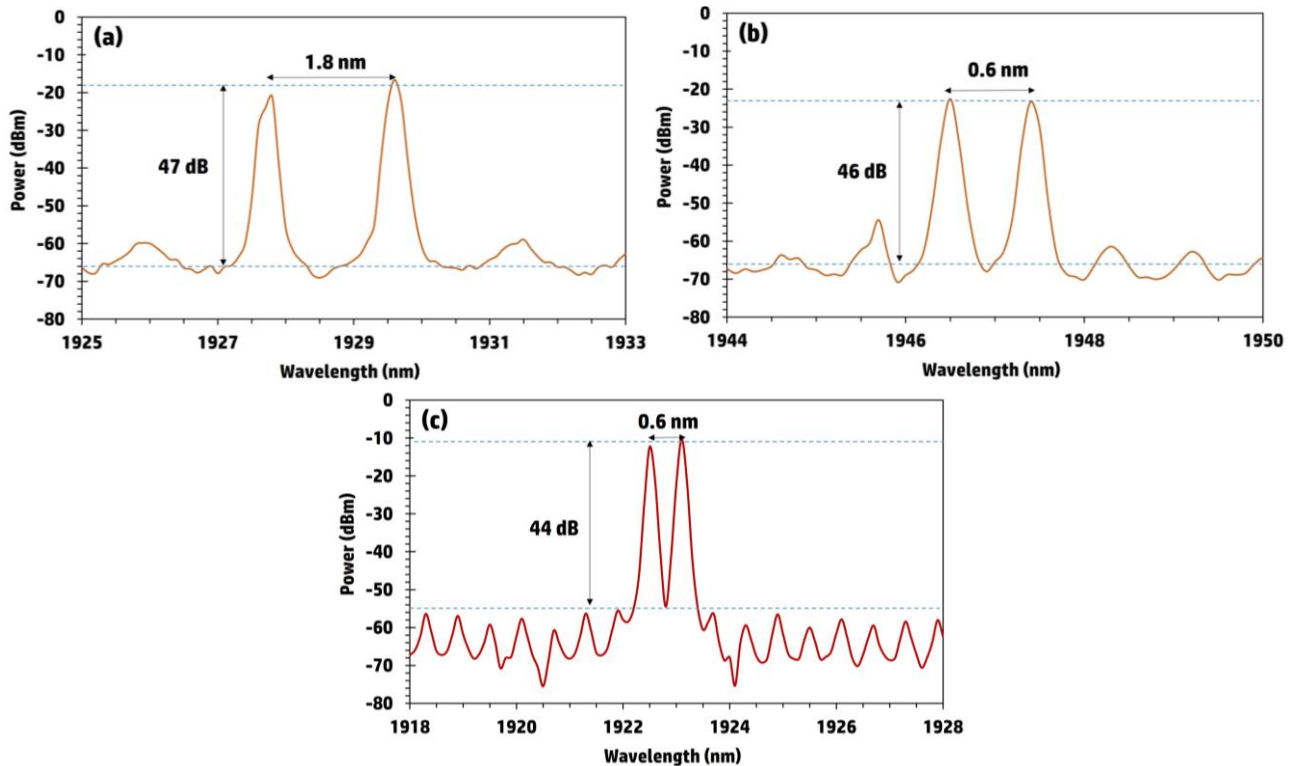


Fig. 4. ER and wavelength spacing of the TDFL based on a Lyot filter at 900 mW for (a) 5 m PMF, (b) 10 m PMF and (c) 15 m of PMF (colour online)

The stability of the TDFL was measured under the optimum conditions of the pump and HWP angles. The output spectrum was observed every one minute in an 8-minute time frame. The wavelength and power variations of the dual-wavelength spectra are shown in Fig. 5. Fig. 5(a) shows the wavelength variation of 1.6 nm for the channel of 1927.9 nm and 1929.7 nm with 5 m PMF, while the power variation is around 11 dB for the former and 6 dB for the latter which can be seen in Fig. 5(b). Fig. 5(c) and 5(d) illustrate the wavelength and power variations for 10 m PMF, respectively. The wavelength shift for output channels 1934.5 nm and 1935.4 nm is 0.5 nm, while the power variation for 1934.5 nm is 2.60 dB and the power variation for 1935.4 nm is 4.69 dB. Lastly, the wavelength and power variations obtained using the 15 m PMF are depicted in Fig. 5(e) and 5(f). The two output channels, 1922.5 nm and 1923.1 nm, have the same wavelength shift of 1.0 nm. In terms of output power variations, the 1922.5 nm channel has a power variation of 9.41 dB, while an output power variation of 13.12 dB was obtained by the 1923.1 nm output. The power variations using the 15 m PMF are the highest compared to that of the 5 m and 10 m PMF. While the power variation is over 12 dB, this result is still acceptable.

In the laser cavity, the PDI and PC provide the IDL mechanism to reduce gain mode competition. In addition, the HNLFF helps to improve the IDL mechanism and increase the stability of the generated dual-wavelength spectra. Despite the high fluctuations in wavelength and power variations, the 10 m of PMF still attained a stable

result. Even with the use of the two nonlinear effects, this shows that environmental conditions also play a role in the stability of the fiber laser. The vibrations surrounding the experimental setup and the temperature of the surrounding cause instability of the fiber laser. Besides that, the fibre's temperature fluctuations and the unstable polarization state of the pump laser can also be detrimental to a fiber laser and cause power fluctuation. These effects cause the polarization state of the fiber laser to be affected. This in turn influences the polarization mode competition, causing fluctuations in power and wavelength [42]. Efficient utilization of pump power requires maintaining a stable temperature by enclosing the fiber laser system in a temperature-controlled chamber. To further enhance stability, environmental vibrations should be minimized by placing the system on an anti-vibration optical table [43]. Determining the optimal TDF length involves securing the fiber in a stable, temperature-controlled environment to prevent fluctuations. Encasing the fiber in a thermal isolation chamber or wrapping it with a thermally conductive material helps ensure consistent performance. Effective heat extraction reduces temperature-dependent losses and enhances laser efficiency [44]. This issue can be mitigated by using a nonlinear optical loop mirror, which helps stabilize the polarization state [45]. Additionally, cooling the PMF in a thermostatic ice bath at a constant temperature has improved lasing stability, as demonstrated in [46]. That said, results such as those obtained using the 15 m PMF can still be considered for applications such as WDM communication and optical sensing.

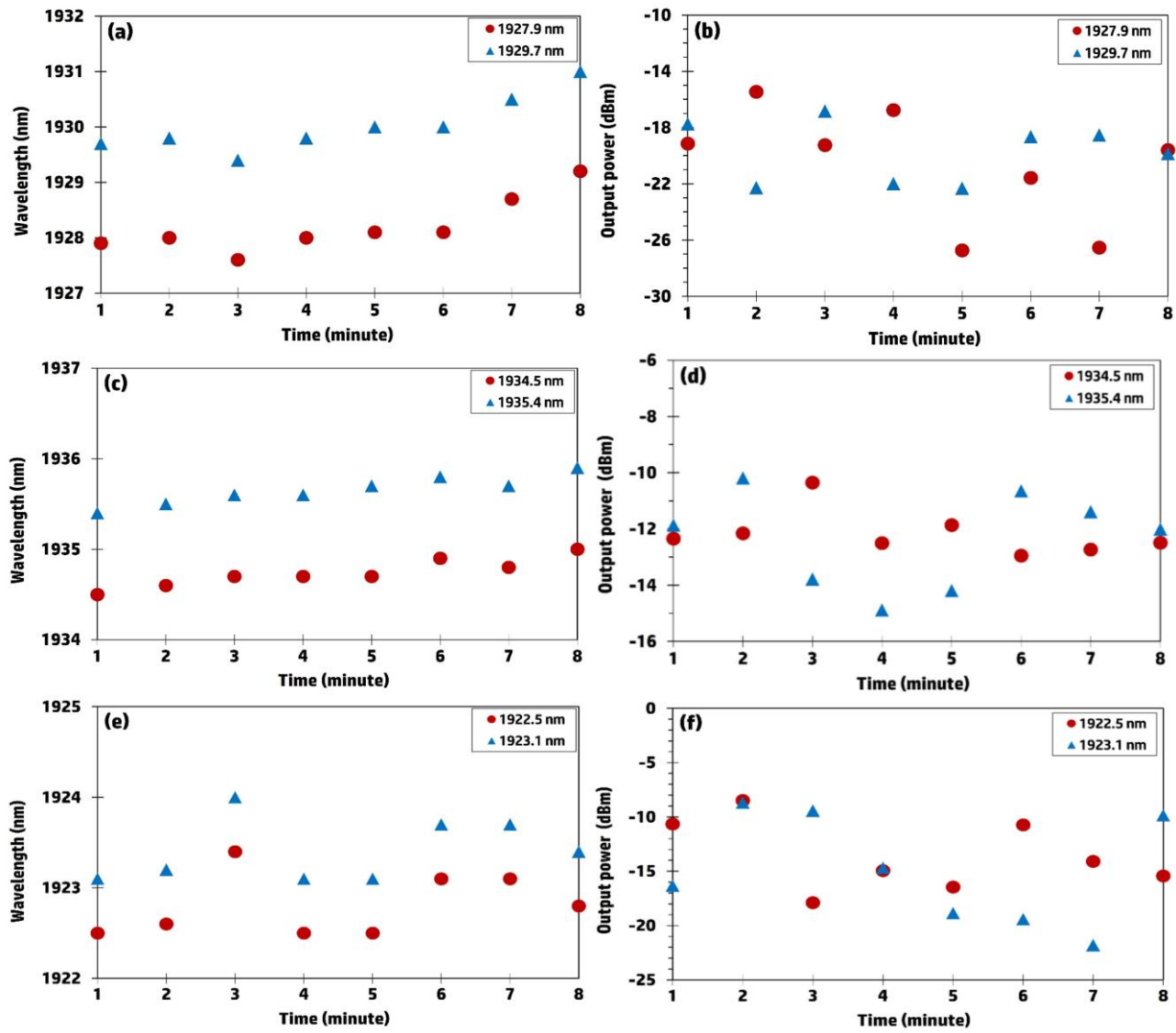


Fig. 5. The observation of wavelength shifting for (a) 5 m, (c) 10 m and (e) 15 m of PMF (colour online)

## 5. Conclusion

We have demonstrated DWTDFL based on Lyot filter in conjunction with IDL mechanism. A Lyot filter at different PMF length was incorporated in the laser ring cavity to act as a comb filter with variation of wavelength spacing. The ER from this experiment reached over 40 dB using a pump power of 900 mW. The wavelength spacing is changed from 1.8 nm to 0.6 nm when different PMF lengths of 5 m to 15 m are applied. From the three PMF lengths, the 10 m PMF has the highest stability in terms of wavelength shift and power variation. This multiwavelength DWTDFL can be utilized for potential applications such as optical sensing, telecommunication, and signal processing.

## Acknowledgements

This research was partly financially supported by the Ministry of Higher Education under the Fundamental Research Grant Scheme (FRGS/1/2020/ICT05/UTM/02/2) and Universiti Teknologi Malaysia under the UTM Fundamental Research (Q.K130000.3856.22H95). This work was also supported by Tenaga Nasional Berhad (TNB) and UNITEN through the BOLD Refresh Postdoctoral Fellowships under the project code of J510050002-IC-6 BOLDREFRESH2025-Centre of Excellence.

## References

- [1] N. Zhang, X. Chen, Y. Yang, H. Sun, Y. Luo, J. Phys.: Conf. Ser. **1812**, 012012 (2021).
- [2] R. Liao, Y. Song, W. Liu, H. Shi, L. Chai, M. Hu,

- Opt. Express **26**(8), 11046 (2018).
- [3] Y. Bai, F. Yan, T. Feng, W. Han, L. Zhang, D. Cheng, Z. Bai, X. Wen, *Optical Fiber Technology* **51**, 71 (2019).
- [4] P. Z. Peng Zhang, W. M. Wanzhuo Ma, T. W. Tianshu Wang, Q. J. Qingsong Jia, C. W. Chunming Wan, *Chinese Optics Letters* **12**(11), 111403 (2014).
- [5] W. He, L. Zhu, M. Dong, F. Luo, *Microw. Opt. Technol. Lett.* **58**(8), 1790 (2016).
- [6] X. Wang, P. Zhou, X. Wang, H. Xiao, L. Si, *IEEE Photonics Journal* **6**(1), 1 (2014).
- [7] A. W. Al-Alimi, M. H. Abu Bakar, N. H. Zainol Abidin, A. F. Abas, M. T. Alresheedi, M. A. Mahdi, *Opt. Laser Technol.* **112**, 26 (2019).
- [8] E. Engels, M. Westlake, N. Li, S. Vogel, Q. Gobert, N. Thorpe, A. Rosenfeld, M. Lerch, S. Corde, M. Tehei, *Biomed. Phys. Eng. Express* **4**(4), 044001-1 (2018).
- [9] S. Maruccia, I. Fulgheri, E. Montanari, S. Casellato, L. Boeri, *Lasers Med. Sci.* **36**(7), 1355 (2021).
- [10] C. R. Wilson, J. D. Kennedy, P. B. Irby, N. M. Fried, *J. Biomed. Opt.* **23**(07), 1 (2018).
- [11] A. Parriaux, K. Hammani, G. Millot, *Opt. Lett.* **44**(17), 4335 (2019).
- [12] J. H. Gene, S. D. Lim, S. K. Kim, *J. Phys.: Conf. Ser.* **1065**(3), 032006 (2018).
- [13] T. Huang, X. Li, P. P. Shum, Q. J. Wang, X. Shao, L. Wang, H. Li, Z. Wu, X. Dong, *Opt. Express* **23**(1), 340 (2015).
- [14] H. Ahmad, M. H. M. Ahmed, M. Z. Samion, S. W. Harun, *Opt. Commun.* **456**, 24589 (2020).
- [15] S. Liu, F. Yan, F. Ting, L. Zhang, Z. Bai, W. Han, H. Zhou, *IEEE Photonics Technology Letters* **28**(8), 864 (2016).
- [16] W. He, L. Zhu, M. Dong, X. Lou, F. Luo, *International Conference on Manipulation, Manufacturing and Measurement on the Nanoscale (3M-NANO)*, 306–311 (2016).
- [17] A. H. Sulaiman, A. P. David, A. Ismail, N. N. Abu Hassan, F. Abdullah, M. Z. Jamaludin, N. Md Yusoff, *Applied Optics* **63**(5), 1241 (2024).
- [18] L. Zhu, W. He, M. Dong, X. Lou, F. Luo, *Modern Physics Letters B* **30**(21), 1650292 (2016).
- [19] B. Sun, J. Luo, Z. Yan, K. Liu, J. Ji, Y. Zhang, Q. J. Wang, X. Yu, *Opt. Express* **25**(8), 8997 (2017).
- [20] M. Wang, Y. J. Huang, J. W. Yang, Y. Zhang, S. C. Ruan, *Laser Phys. Lett.* **15**(8), 085110 (2018).
- [21] Y. Wei, K. Hu, B. Sun, T. Wang, *Laser Phys.* **22**(4), 770 (2012).
- [22] Y. Wei, X. Yang, B. M., Mao, Y. Lu, X. Zhou, M. Bi, G. Yang, *Microw. Opt. Technol. Lett.* **58**(2), 337 (2016).
- [23] D. Liu, N. Q. Ngo, X. Y. Dong, S. C. Tjin, P. Shum, *Appl. Phys. B* **81**(6), 807 (2005).
- [24] R. M. Sova, C.-S. Kim, J. U. Kang, *IEEE Photonics Technology Letters* **14**(3), 287 (2002).
- [25] N. H. Zainol Abidin, M. H. Abu Bakar, N. Tamchek, F. R. Mahamd Adikan, M. A. Mahdi, *Opt. Express* **26**(12), 15411 (2018).
- [26] F. Wang, Y. Gong, *IEEE Access* **8**, 218614 (2020).
- [27] X. Mao, F. Yan, L. Wang, S. Feng, J. Peng, S. Jian, *Opt. Commun.* **282**(1), 93 (2009).
- [28] Y. S. Ong, A. H. Sulaiman, F. Abdullah, K. Y. Lau, N. M. Yusoff, *International Journal of Integrated Engineering* **12**(6), 273 (2020).
- [29] A. P. Luo, Z. C. Luo, W. C. Xu, V. V. Dvoyrin, V. M. Mashinsky, E. M. Dianov, *Laser Phys. Lett.* **8**(8), 601 (2011).
- [30] H. Shawki, H. Kotb, D. Khalil, *OSA Contin.* **2**(2), 358 (2019).
- [31] Y. Xu, L. Zhang, L. Chen, X. Bao, *Opt. Express* **25**(14), 15828 (2017).
- [32] H. Zou, S. Lou, W. Su, B. Han, *Laser Phys.* **24**(5), 055102 (2014).
- [33] G. Lu, F. G. Sun, G. Z. Xiao, C. P. Grover, *IEEE Photon. Technol. Lett.* **4**(6), 1280 (1992).
- [34] N. Md. Yusoff, L. K. Yao, A. H. Sulaiman, N. Mohd Yusoff, M. A. Mahdi, *Opt. Laser Technol.* **135**, 106707 (2021).
- [35] M. A. Umyy, N. Madamopoulos, M. Razani, A. Hossain, R. Dorsinville, J. Y. W. Lee, B. Jung, *Opt. Express* **20**(1), 23367 (2012).
- [36] J. Swiderski, M. Maciejewska, W. Pichola, J. Kwiatkowski, M. Mamajek, *Laser Technology: Progress in Lasers* **8702**, 119 (2013).
- [37] S. Liu, F. P. Yan, B. L. Wu, S. Y. Tan, W. J. Peng, T. Feng, X. Liang, Q. Li, *Journal of Optics* **16**(5), 055201 (2014).
- [38] R. Paschotta, *RP Photonics Encyclopedia*, (2023).
- [39] Q. Zhao, L. Pei, J. Zheng, M. Tang, Y. Xie, J. Li, T. Ning, *Journal of Lightwave Technology* **37**(15), 3784 (2019).
- [40] H. E. M. Aliza, A. H. Sulaiman, N. M. Yusoff, M. Z. Jamaludin, F. Abdullah, A. Ismail, A. P. David, A. A. A. Lah, *International Conference on Computer and Communication Engineering (ICCCE)*, 425 (2023).
- [41] K. Scholle, S. Lamrini, P. Koopmann, P. Fuhrberg, *Frontiers in Guided Wave Optics and Optoelectronics*, B. Pal, Ed., InTech, 2010.
- [42] X. Wang, Y. Zhu, P. Zhou, X. Wang, H. Xiao, L. Si, *Opt. Express* **21**(22), 25977 (2013).
- [43] E. K. Kashirina, I. A. Lobach, S. I. Kablukov, *Photonics* **11**(8), 731 (2024).
- [44] M. Eilchi, P. Parvin, *Heat Generation and Removal in Fiber Lasers, Fiber Laser*, InTech, 2016.
- [45] T. Li, F. Yan, P. Wang, X. Wang, Y. Suo, H. Zhou, *Infrared Phys. Technol.* **125**, 104269 (2022).
- [46] Z. Zhao, X. Li, Y. Li, H. Qin, H. Wang, Y. Luo, Z. Yan, Q. Sun, D. Liu, L. Zhang, *Appl. Opt.* **57**(31), 9270 (2018).

\*Corresponding author: nelidya.kl@utm.my;  
hadisulaiman@usm.my